JOURNAL OF SOLID STATE CHEMISTRY 102, 455–464 (1993)

Band Gap Closing in $La_{2-x}Sr_xNiO_{4+\delta}$

X. GRANADOS,* J. FONTCUBERTA,* M. VALLET-REGÍ,† M. J. SAYAGUÉS,‡ AND J. M. GONZÁLEZ-CALBET‡

*I.C.M.A.B.-C.S.I.C., Campus Universitat Autònoma Barcelona, 08193 Bellaterra, Barcelona, Spain; †Laboratorio de Magnetismo Aplicado (RENFE-UCM), 28290 Las Matas, Madrid, Spain; and ‡Departamento de Química Inorgánica, Universidad Complutense, 28040 Madrid, Spain

Received November 12, 1991; in revised form July 9, 1992; accepted July 14, 1992

Structural and electrical transport measurements are reported for the layered $La_{2-x}Sr_xNiO_{4+\delta}$ oxide for a range of Sr and oxygen contents. The electrical properties change from semiconductor-like for $x < 0.8$ to metallic for larger Sr content. The room temperature Seebeck coefficient changes from semiconducting and positive for small x toward metallic and negative for large doping levels. From analysis of the temperature dependence of the Seebeck coefficient we conclude that the transition from the semiconductor to the metallic side of the phase diagram is achieved by the closing of the band gap. © 1993 Academic Press, Inc.

1. Introduction

Transport and magnetic properties studies of K_2NiF_4-type oxides are subjects of current interest for a number of reasons. The occurrence of superconductivity in the La_2CuO_4 member of this family is an important one, but the change from semiconducting to metallic behavior observed at high temperature or when the sample is conveniently doped are interesting in itself.

Before the discovery of superconductivity in the La–Sr–Cu–O system, oxides of K_2NiF_4 structure were already interesting because of the strong anisotropy of the structure which leads to a an essentially $2D$ oxide. Special attention has been devoted to the La_2NiO_4 oxide, its transport, magnetic, and structural properties (*1–4*). However, much less attention has been paid to the Sr-substituted $Ln_{2-x}Sr_xNiO_4$ (Ln = La, Nd, . . .) oxide in spite of its close structural similarity to the superconducting cuprates.

Khairy *et al.* (*5*) reported the transport properties of $La_{2-x}Sr_xNiO_4$ ($x < 1.12$) in the high temperature regime 300–1200 K. They found that the resistivity decreases with x, and there is a progressive transition from semiconductor-like behavior to metallic behavior at high temperature.

Recently, Takeda *et al.* (*6*) and Cava *et al.* (*7*) have reported electrical measurements on samples of well defined oxygen content down to 10 K. It was found that the semiconductor–metal transition temperature decreases monotonically with increasing x from about 675 K ($x = 0$) to 20 K ($x = 1.2$). The room temperature Hall coefficient was found (*6*) to change from positive for $x > 1$ to negative for $x < 0.6$. The observation of a negative Hall coefficient for the

0022-4596/93 $5.00

low-doped $La_{2-x}Sr_xNiO_4$ sample is surprising in view of the well established p-type conductivity in the nondoped samples of La_2NiO_4. It is also disturbing that the reported Hall coefficient increases when x increases (for $x > 1$) thus indicating a lowering of the hole concentration.

It is clear that extensive efforts are needed to get a comprehensive understanding of the transport properties; in particular, the character of the metal–insulator (M–I) transition and the sign of the majority charge carriers are still open questions. To that purpose, we report in this paper new experimental data on a set of well characterized $La_{2-x}Sr_xNiO_4$ samples. Of particular relevance are the temperature dependence of the Seebeck coefficient data which provide new clues in regard to the origin of the I–M transition.

2. Experimental

Two series of samples (R and O) of $La_{2-x}Sr_xNiO_{4+\delta}$ were prepared from stoichiometric mixtures of dried La_2O_3, $SrCO_3$, and NiO. Samples of series O were obtained by oxidation in air at 1200°C and samples of series R were first reduced under Ar (results for these reduced samples have been reported elsewhere (*8*) and later were reoxidized by flowing oxygen at 1000°C for 24 hr. From iodometric titration it turned out that the concentration of $(NiO)^+$ units in both series of samples was essentially coincident. Although it is well known that iodometric titration alone cannot provide an accurate measure of the oxygen content in the sample, especially if the possibility of the existence of O^- species is considered (*9*), it can be used to compare both sets of samples. In Fig. 1, we show a rough estimation of the oxygen excess (δ) deduced from the electroneutrality condition (assuming O^{2-}), the cation composition, and the $(NiO)^+$ content deduced from the iodometry. The data in Fig. 1 clearly reveal that for a given Sr concentration, the samples of O and R series have similar oxygen contents.

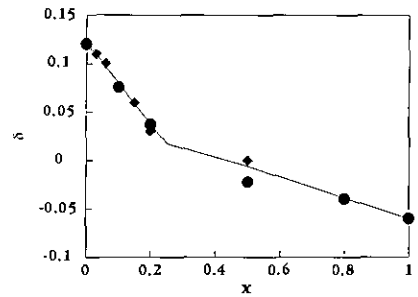

FIG. 1. Oxygen excess (δ) as a function of Sr concentration (x). Squares and circles correspond to samples from the R and O series, respectively.

Powder X-ray diffraction patterns were obtained on a Siemens diffractometer by using Cu$K\alpha$1 radiation. Intensity data were collected each 0.02° step in the angular range $20° < 2\Theta < 100°$. Cell parameters and atomic positions were obtained by using the *I4/mmm* space group and the Rietveld method.

Cylindrical pellets of sizes $D = 13$ mm, $h = 2$ mm and $D = 6$ mm, $h = 0.3$ mm were prepared from powders of series O and R, respectively. After pelletizing and sintering, the samples of the R and O series have compactness between 60% and 70% and between 75% and 80%, respectively. Rectangular bars ($1 \times 1 \times 10$ mm^3) were cut from the pellets of O samples and the original cylindrical pellets of samples of R series were used to perform electrical resistance measurements by the four-probe method, from 10 to 300 K. For the more resistive samples ($x \leq 0.5$) only the 60–300 K temperature range has been investigated. At lower temperature the higher resistivity of the sample makes the measurements to be not reliable because of the input impedance of the voltmeter. A test of linearity was performed to ensure ohmic behavior of the contacts (silver paint). Data were corrected for 100% compactness using the Landauer expression (*10*).

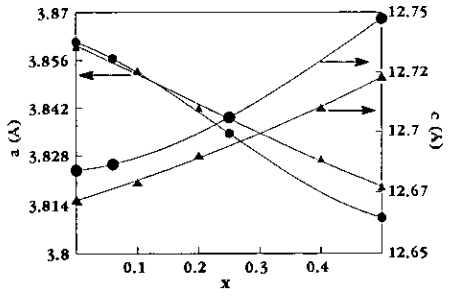

FIG. 2. Tetragonal lattice parameters $a(x)$ and $c(x)$. The circles are our own results. The results of Khairy *et al.* (*5*) (triangles) are also shown.

The Seebeck coefficient in the 300–80 K temperature range was measured by a differential method with a reproducibility better than 10% using a homemade apparatus.

As stated above, samples of batches O and R have no differences in oxygen content. It will be shown below that they also have the same composition and temperature dependencies of the resistance. The Seebeck coefficient values are also coincident. Samples of O and R series differ only in the absolute value of the measured resistance. This difference is caused by the presence of microscopic cracks existing in the sample (*7*) which can be more important for pellets of batch R because of their smaller size. The existence of cracks and grain boundaries is more relevant in resistivity than Seebeck measurements because of the open circuit experimental conditions of the latter. Consequently, we will not attempt to compare the absolute values of the resistivities but will use only the temperature and composition dependence of the measured resistance in the discussion of the experimental data.

3. Results and Discussion

3.1. Lattice Parameters

Figure 2 shows the tetragonal lattice parameters a and c as a function of the strontium content (x). The parameter a decreases monotonically as x increases while the parameter c increases. The data of Khairy *et al.* (*5*) are also included for comparison. The fact that the slope of $a(x)$ does not change appreciably where the slope of the $\delta(x)$ curve clearly changes ($x = 0.2$, see Fig. 1) indicates that this cell parameter does not depend much on the oxygen content. As shown in Fig. 2 the c parameter is more sensitive to the oxygen content.

The stability of the K_2NiF_4 structure is commonly described in terms of the tolerance factor

$$t = \frac{r_{A-O}}{r_{B-O}\sqrt{2}}$$

where $r_{A-O} = r_A + r_O$ and $r_{B-O} = r_B + r_O$ refer to the sum of the ionic radii of oxygen and A and B cations. A and B cations have coordination numbers of 9 and 6, respectively. The tetragonal K_2NiF_4 is stable for $0.85 < t < 1$. For the stoichiometric La_2NiO_4 oxide, $t \approx 0.88$, which is close to the lower limit, thus explaining why the ideal tetragonal structure is somewhat distorted. For $x > 0$, t increases for two reasons. First, the substitution of the La^{3+} by the larger Sr^{2+} ion increases r_{A-O} and thus t. Second, stability can be increased by reducing the r_{B-O} distance; this effect can be accomplished by oxidizing the transition metal cation to a higher valence state. For instance, oxygen rich $La_2NiO_{4+\delta}$ oxide, formally containing Ni^{3+}, is tetragonal.

Figure 1 suggests that the $x < 0.2$ stabilization of the tetragonal structure results from both Sr^{2+} ion size and oxygen excess effects. For $x \geq 0.2$, the slope of $\delta(x)$ is smaller, indicating that charge neutrality and structure stabilization are basically achieved by Sr^{2+} and Ni^{3+} size and charge effects; oxygen defect plays a minor role. The data of Figure 1 illustrate that the binding energy of interstitial oxygen is smaller than that of the oxygen ions in the lattice sites.

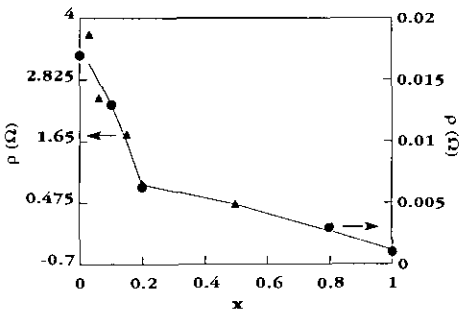

FIG. 3. Room temperature electrical resistance versus the Sr contents (x) for samples of both series O (circles) and R (triangles). The right and left Y-axes correspond to the O and R series, respectively.

3.2. Room Temperature Resistance

Figure 3 is a plot of the room temperature DC resistance (ρ) versus x, for $La_{2+x}Sr_xNiO_{4+\delta}$ samples of series O and R. Both sets of data show the same behavior: the resistance decreases when the Sr content increases. For $x > 0.2$ the resistance appears to be less sensitive to the Sr content.

Comparison of Fig. 3 and Fig. 1 reveals that the changes of slopes of $\rho(x)$ and $\delta(x)$ observed at $x \approx 0.2$ are closely related. For $x > 0.2$ the enhanced conductivity is mainly caused by the holes introduced into the Ni–O layers by the Sr doping. The absolute value of resistivity measured in ceramic materials is subject to a number of experimental limitations (*16*) which are difficult to overcome. Therefore, comparison of the absolute values can be meaningless. However, it is worth to recognize that the resistivity that one can extract from our data is close (within an order of magnitude) to previously reported values and the room temperature resistance vs compositions is also similar to that found by others (*5–7, 11–14*).

Arbukle et al. (*15*) reported resistivity measurements in the very similar oxide $Nd_{2-x}Sr_xNiO_{4+\delta}$. The general behavior of $\rho(x)$ is similar to that shown in Fig. 3. In close agreement with the present data, a faster decrease of $\rho(x)$ for $x < 0.2$ than for larger x values was also observed. It is worth noticing that in the $Nd_{2-x}Sr_xNiO_{4+\delta}$ case, the change of behavior of $\rho(x)$ occurs also at $x = 0.2$.

3.3. Temperature Dependence of Electrical Resistance ($T < 300$ K)

In Fig. 4 we show the plot of $\log(\rho)$ vs $1/T$ for some representative $La_{2-x}Sr_xNiO_{4+\delta}$ compositions in the 60–300 K temperature range. The $x = 0.8$ and $x = 1$ samples display metallic behavior above a certain temperature (≈200 K for $x = 1$). For $x < 0.8$ all members of these series are semiconductors in the explored temperature range. For the low-doped samples ($x < 0.5$) a linear fit of the $\log(\rho)$ vs. $(1/T)$ curves in the high temperature region ($T > T^* \approx 110$ K) gives activation energies (E_σ) in the 70–90 meV range. The values of E_σ do not depend much on the alkaline earth content. For $x \approx 0.5$ a single activation energy cannot be obtained because of the pronounced curvature of $\log(\rho)$ vs $1/T$.

An order of magnitude of the mobility at room temperature can be obtained from the measured resistivity and using the doping level as measure of the charge carrier concentration. In ceramic materials the measured resistivity represents only an upper limit for the actual resistivity value (*16*). Consequently, to deduce an estimate of the mobility we use the resistivity measured for

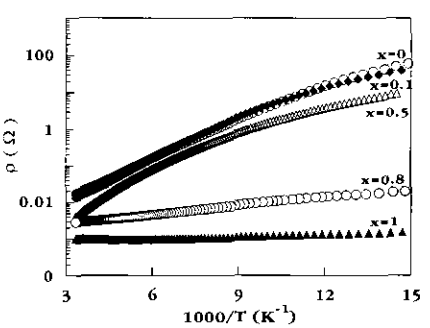

FIG. 4. Log(ρ) vs $1/T$ for some samples of series O.

the O series because its lower values should be closer to the actual one. For $x = 0.03$ the hole concentration deduced by iodometry is $p(0.03) = 2.6 \times 10^{21}$ cm^{-3} and the room temperature resistivity is about 0.020 Ω cm; the mobility results to be $\mu(300\ \text{K}) = 0.12$ cm^{2}V^{-1} sec^{-1}. This small value of the mobility indicates that either the valence band is very narrow or there is some degree of localization. In the perovskite $La_{1-x}Sr_xVO_3$, the high temperature (800 K) mobility for the semiconducting composition range was found to be $\mu = 1.5 \times 10^{-1}$ cm^{2}V^{-1}s^{-1} (*17*). Our mobility for $x \approx 0.03$ is of the order of the limiting value of 0.1 cm^{2}V^{-1}sec^{-1} suggested by Mott and Davis (*18*) for hopping conduction just above a mobility edge. If one uses the free electron mass value, a mobility of about 1 cm^{2}V^{-1} sec^{-1} should be used to obtain an estimation of the carriers mean free paths of the order of the interatomic distances. Our smaller value signals an important enhancement of the effective mass.

At temperatures below T^*, there is a progressive lowering of the slope of log(ρ) vs $1/T$ thus indicating that at low temperatures the transport properties are dominated by a different conduction mechanism. The curvatures of log(ρ) vs $1/T$ do not change appreciably with x. This observation suggests that low temperature resistivity is controlled by similar extrinsic defects. The general behavior of $\rho(T)$ is very similar to that recently reported for $Nd_{2-x}Sr_xNiO_{4+\delta}$ (*15*).

We have mentioned above that for $T < T^*$ a new conducting channel should be open to account for the apparent lowering of the slope of log(ρ) vs. $1/T$. A contribution of a VRH (Variable Range Hopping) regime is explored in Fig. 5, where log(ρ) is plotted vs $(1/T)^{1/4}$. Within a 3D VRH model a $\rho = \rho_0 \exp(T_0/T)^{1/4}$ dependence is expeeted. Figure 5 shows that the VRH law fits the data reasonably well, thus suggesting that in the low temperature range (160 K > T > 60 K)

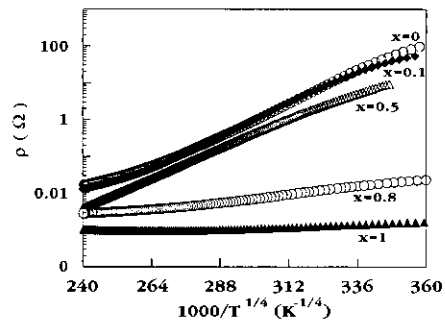

FIG. 5. Log(ρ) vs $(1/T)^{1/4}$ for some samples of series O.

the variable range hopping model can be used to account for the data. Obviously, this fit becomes gradually meaningless as x increases and the metallic regime is approached ($x > 0.8$).

3.4. *Thermoelectric Effects*

The room temperature dependence of the Seebeck coefficient (S) on the Sr content is summarized in Fig. 6. For low-doped samples S is positive and decreases as x increases. It becomes negative at $x \approx 0.15$ and reaches a minimum value at $x \approx 0.6$. At higher doping S increases again but it remains negative up to $x = 1$. Previous measurements of the thermopower by Gopalakrishnan *et al.* (*14*) found similar results. Our data for $x = 0$ are also in good agreement with the reported value of S (=5 μV/K) for La_2NiO_4 single crystals (*19*). It is not surprising that the Seebeck coefficient for single crystal and our polycrystalline materials are in such close agreement because the experimental open-circuit measuring condition makes the thermopower measurements much less sensitive to the granular character of the samples.

Shown in Fig. 7a is the temperature dependence of $S(T)$ for $La_{2-x}Sr_xNiO_{4+\delta}$ in the 70–300 K temperature range. All semiconducting samples display the same general behavior; i.e., when temperature decreases the Seebeck coefficient increase, reaching

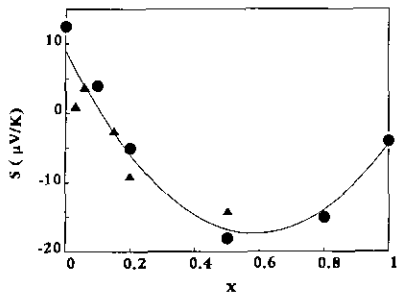

FIG. 6. Room temperature Seebeck coefficient for $La_{2-x}Sr_xNiO_{4+\delta}$ for samples of the O series (circles) and of the R series (triangles).

a maximum at certain temperature T_M and decreasing again for lower temperatures. At room temperature S is already negative for $x > 0.15$ but for all compositions $S(T)$ also extrapolates to negative values at higher temperatures. For $x \geq 0.8$, $S(T)$ is quasi-linear and negative, signaling the onset of a metallic conductivity dominated by electron-like charge carriers. For $x = 0.8$ the low temperature decrease of $S(T)$ is reminiscent of the semiconductor behavior observed in $\rho(T)$. In Fig. 7b, $S(T)$ data are plotted vs $1/T$. From this plot it can be appreciated that the low-doped samples show thermally activated behavior for $T > T_s(x) > T_M$, in agreement with classical theory of excitation of carriers from localized levels to a conduction band. In such a case, S is given by

$$S \approx k/e((E_F - E_v)/kT + A), \qquad (1)$$

where A is a parameter reflecting the scattering process and the temperature dependence of the band gap. In Table I we summarize the activation energies $E_s = E_F - E_v$ deduced from the fit of data to Eq. (1) together with the temperature (T_s) which signals the onset of the activated regime given by Eq. (1). Because of the narrow temperature interval where the activated behavior is observed the extracted energies should be considered only as a rough estimate.

The activation energies E_s obtained from the data of Fig. 7b are always remarkably smaller than the corresponding energies obtained from conductivity measurements. The energy differences $E_\mu = E_\sigma - E_s$, also included in Table I, are about 60–80 meV. Large E_μ values may indicate the important contribution of the polaron energy formation in the mobility of the charge carriers. Table I also shows that $A < 0$ for all the samples. The A term must be positive if it includes only the scattering process (*20*). Negative A values can be originated by a contribution from the temperature dependence of the band gap. If one assumes a linear temperature-dependent band gap, $E_F - E_v = \Delta_E - \gamma T$ and consequently $A = A_0 - \gamma/R$, where A_0 is the scattering contribution. Furthermore, if scattering by charged impurities is the dominant mechanism, then $A_0 = 4$ (*20*) and from the data

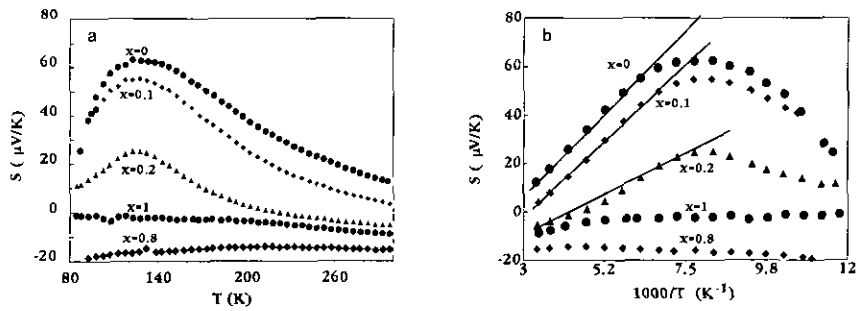

FIG. 7. (a) Temperature dependence of the Seebeck coefficient, and (b) plot of S vs $1/T$ for several O samples. Linear behavior is observed above a certain temperature, T_s, which depends on x.

TABLE I

ENERGIES DEDUCED FROM RESISTANCE DATA (E_σ) AND FROM SEEBECK DATA (E_S), MOBILITY ENERGIES ($E_\mu = E_\sigma - E_S$), MINIMUM TEMPERATURE (T_S, SEE TEXT), AND THE A COEFFICIENT IN EQ. (1)

X	Series	E_σ(meV)	E_S(meV)	E_μ	T_S(K)	A
0	O	73	14	59	157	−0.46
0.03	R	80	13	60	152	−0.55
0.06	R	70	10	70	125	−0.35
0.1	O	80	14	66	151	−0.54
0.15	R	72	9	80	144	−0.46
0.2	R	90	11	80	150	−0.66
0.2	O	90	7.1	72	128	−0.39

of Table I, values of γ ranging from 3.7×10^{-4} to 4.5×10^{-4} eVK^{-1} are determined. These values are similar to those found for $La_{1-x}Sr_xVO_3$ by Webb *et al.* (*17*). It is also similar to the value that can be inferred from the Seebeck results on La_2NiO_4, reported by Sayer *et al.* (*13*).

At temperatures $T < T_S \approx 100$K, the Seebeck coefficient decrease again. If according to the discussion of Section 3.3 at low temperature a VRH mechanism holds, an $S \approx \sqrt{T}$ dependence is expected (*18*). On the other hand, starting from the low temperature side of the $S(T)$ curve, a gradual increase of S is also characteristic of an extrinsic semiconductor in the temperature range where the minority carriers are negligible. In this case, $S(T)$ rises because of the increasing effective density of states and a $S(T) \propto \mathrm{Ln}(T)$ dependence is expected (*15*). Our data roughly display this temperature dependence. However, on the basis of the present Seebeck data, the investigated temperature range below 100 K is to narrow to dilucidate between both mechanisms.

An alternative explanation for $A < 0$ is as follows. Negative A results from the experimental observation that for any composition at high temperature $S(T)$ extrapolates to negative values. It is important to observe that $S(T)$ becomes negative at lower temperature as x increases (see Fig. 7a). It is well known that in p-doped Ge or Si (*21*) the Seebeck coefficient is positive at low temperatures but at high temperatures the intrinsic conductivity dominates the electrical response of the material and S becomes negative. Similarly, one can argue that in $La_{2-x}Sr_xNiO_{4+\delta}$ for low-doped samples and at relatively low temperatures, the Sr substitution or the native excess of oxygen gives rise to an extrinsic conductivity and a positive Seebeck coefficient. At higher temperatures the intrinsic conductivity sets in and because of the higher mobility of the electrons with respect to holes (*20*) the sign of S becomes negative. Consequently, S is electron-like at high temperature. Note that with this approach, the enhancement $S(T)$ in the 300–100 K temperature range does not provide a simple measure of either the activation energy or the band gap because in this transition region from intrinsic to extrinsic conductivity, the Seebeck coefficient is strongly dependent on the relative mobility of both electrons and holes and on their concentrations (*21*). If so, the activation energies E_σ and E_μ of Table I could not be significant.

Within this framework, the fact that for heavily doped samples the room temperature Seebeck coefficient is already negative may indicate that for these samples the intrinsic regime is reached at lower tempera-

tures and consequently we can conclude that the band gap should become narrower as x increases.

4. Concluding Remarks

In the simplest approximation of a single parabolic band, the positive Seebeck coefficient data for the low level doping samples, which have excesses of oxygen, signals that holes are present in the sample and dominate the transport properties. Excess oxygen, probably as interstitial O_2^{-1} as found in La_2CuO_4 (*9, 22*), acts as an acceptor level ($A°(O)$) in the electronic band gap of the material. The partial substitution of La by Sr also creates acceptor levels ($A°(Sr)$) above the VB (valence band). At 0 K holes are bound to the acceptor levels but at higher temperatures an electron can be excited from the VB to these levels, thus leading to a hole that can move "freely" in the VB.

Recent results on Li-doped NiO oxides (*23*) have shown that holes reside primarily on the oxygen $2p$ orbital rather than on the metal orbitals. Recently, a similar suggestion has been made for $La_2NiO_{4+\delta}$ and $La_{2-x}Sr_xNiO_{4+\delta}$ (*24*) on the basis of XANES and magnetic susceptibility data. If so, $La_{2-x}Sr_xNiO_4$ should be considered a charge-transfer insulator, with a VB arising essentially from O2p orbitals and a CB arising primarily from Ni3d states.

The most straightforward interpretation of the high temperature regime ($T > 100$ K), where both $\rho(T)$ and $S(T)$ show simply activated behavior, is that we are in an extrinsic region, so the transport properties of the system are dominated by the ionization of the impurities and thus by the thermal activation of holes. $E_A = 2E_s \simeq 26$ meV can be estimated from the activation energy deduced from the Seebeck coefficient of the less doped sample (see Table I). As a result of the interaction of impurity states, the measured activation energy reflects the energy position E_A only in the isolated impurity limit.

The microscopic nature of the activated mobility given by E_μ is far from clear. However, we may tentatively propose the following mechanism. At high temperatures direct excitation of electrons from the VB into the CB states may occur. At lower temperatures excitations can only occur to the localized states (E_A). The hole concentration will be

$$p = p_0 \exp(-(E_A - E_F)/kT),$$

where $E_A - E_F$ is the minimal activation energy necessary to create a hole. As far as this hole is created in the localized levels that should exist close to the top of the VB, it does not contribute to the conductivity. Extra energy ΔW_1 is required to hop from localized site to site, so the mobility will be

$$\mu = \mu_0 \exp(-\Delta W_1/kT).$$

Consequently

$$\sigma = \sigma_0 \exp(-(E_A - E_F + \Delta W_1)/kT)$$

and the measured activation energy from the conductivity measurement will be much larger than that measured from Seebeck data. This is the dominant conduction mechanism above $T > T_s \approx 100$ K. Within this extrinsic conductivity model, the observation of $A < 0$ in Eq. (1) has been interpreted in terms of a temperature-dependent band gap.

Because of E_σ and E_μ do not change appreciably with the Sr contents, even when the (I–M) transition is approached, it appears that the metallic regime is established by charge delocalization within the impurity band.

At still lower temperatures, electrons can be excited to states close to E_F, which are also localized in nature, and can tunnel to more distant sites; this is the VRH regime. From the data presented in Section 3.2 it appears that for the low-doped samples, at

$T < T^*$ (100 K) a VRH model can account for all available data.

However, we have also shown that for $T > 100$ K the $S(T)$ dependence for all semiconducting samples can be understood in terms of a transition from an extrinsic, hole-dominated conductivity, to an intrinsic regime at higher temperature. In the intrinsic region, the higher mobility of electrons excited across that band gap gives rise to a negative Seebeck coefficient. Within this approach it is clear that our results signal that when the Sr concentration increases, the region where intrinsic conductivity dominates the electrical properties of the material is shifted toward lower temperatures. Consequently, we can conclude that the band gap closes as the I–M transition is approached.

A comment on the temperature (T_M) where $S(T)$ reaches its maximum value is in order. Our experimental data hardly reveal any shift of T_M with x. If the intrinsic regime is reached at lower temperatures with increasing Sr contents, at first glance one would expect T_M to be reached at lower temperatures, in contrast with the observed behavior. However, it must be recalled that T_M is the result of a contribution of the low temperature nonintrinsic regime and the high temperature intrinsic one. Although decreasing the band gap would shift the high temperature regime to lower temperatures it may well occur that the low temperature contribution is also reduced thus leading T_M almost unchanged.

On the basis of the present data alone we can not go further in the analysis of the experimental data and so our suggestion of a band gap closing induced by the Sr contents should be only considered as a very plausible explanation of the available experimental results.

The consideration of the extrinsic conductivity model described above was based on the observation of an activated regime for both $\rho(T)$ and $S(T)$. However, the data of Figs. 4 and 7 can be seriously criticized because of the narrow temperature interval where the activated behavior is observed. The alternative picture of a gradual transition from extrinsic to intrinsic behavior at $T > 100$ K avoids this difficulty and explains naturally the curvature observed in $\rho(T)$ for the heavily doped samples.

In some recent papers, Torrance and coworkers (*25*) have shown that in $LnNiO_3$ (Ln = Nd, Sm, Pr) an I–M transition exists at $T \geq 130$ K. These transitions have been interpreted as a result of the closing of the energy gap because of some delicate change of the Ni–O–Ni angles and distances. In the present case, the shortening of the Ni–O–Ni distances could be also at the origin of the I–M transition. However, in $LnNiO_3$ oxides, because of the first-order character of the M–I phase transition, which is accompanied by a sudden change of the cell parameters (*25, 26*), the resistivity change is more abrupt than in $La_{2-x}Sr_xNiO_{4+\delta}$.

In summary, we have reported new resistance and Seebeck data for $La_{2-x}Sr_xNiO_{4+\delta}$. The electrical resistance decreases as the Sr content increases and changes from semiconductor-like to metallic at $x \approx 0.8$. The Seebeck coefficient changes from semiconductor-like to metallic. At room temperature hole-like charge carriers dominate the electrical response of the material for low doping but for larger doping electron-like conductivity sets in. On the basis of the composition and temperature dependence of the Seebeck coefficient we have concluded that the I–M transition is achieved by a band gap closing. At low temperatures and for low-doped samples evidence is found for charge carrier localization and it is argued that disorder introduced by substitutional (Sr) and interstitial (O) species can be its source.

Acknowledgments

We thank the Ministerio de Educación y Ciencia (CICYT) and the MIDAS program (SPAIN) for provid-

ing financial support for this research through Projects MAT-88-0163-C03 and MAT-91-0742.

Note added in proof. After this paper was submitted, we became aware of a recent paper by Th. Strangfeld *et al.* (*27*) reporting resistivity and Seebeck data for $La_{2-x}Sr_xNiO_4$. Their experimental data for $\delta(x)$, $\rho(x)$, and $S(x)$ are in close agreement with the present data.

References

1. C. N. R. Rao *et al., J. Solid State Chem.* **51,** 266 (1984).
2. P. Odier, Y. Nigara, J. Coutures, and M. Sayer, *J. Solid State Chem.* **56,** 32 (1985); F. Gervais, P. Odier, and Y. Nigara, *Solid State Commun.* **56,** 371 (1985).
3. R. Sáez-Puche, J. L. Rodríguez, and F. Fernández., *Inorg. Chim. Acta* **140,** 151 (1987); J. M. Bassat *et al., Phys. Rev. B* **35,** 7126 (1987).
4. X.-X. Bi, P. C. Eklund, E. McRae, Ji-Guang Zhang, P. Metcalf, J. Spalek, and J. M. Honig, *Phys. Rev. B* **42,** 4756 (1990).
5. M. Khairy, P. Odier, and J. Choisnet, *J. Phys. (Les Ulis, Fr.)* **47,** C1–831 (1986).
6. Y. Takeda, R. Kanno, M. Sakano, O. Yamamoto, M. Takano, Y. Bando, H. Akinaga, K. Takita, and J. B. Goodenough, *Mater. Res. Bull.* **25,** 293 (1990).
7. R. J. Cava, B. Batlogg, T. T. Palstra, *et al., Phys. Rev. B* **43,** 1229 (1991).
8. X. Batlle, J. L. García-Muñoz, M. Medarde, J. Rodríguez-Carvajal, X. Obradors, J. L. Martínez, M. Vallet, J. González-Calvet, M. J. Sayagués, and J. Fontcuberta, *Physica C* **162–164,** 1273 (1990); X. Granados, X. Batlle, M. Medarde, X. Obradors, J. Fontcuberta, J. Rodríguez, M. Vallet, J. González-Calvet, J. Alonso, and M. J. Sayagués, *J. Less-Common Met.* **164–165,** 853 (1990).
9. C. N. R. Rao, P. Ganguly, M. S. Hedge, and D. D. Sarma, *J. Am. Chem. Soc.* **109,** 6893 (1987).
10. R. Landauer, *J. Appl. Phys.* **23,** 779 (1952).
11. S. A. Hoffman, C. Venkatraman, S. N. Ehrlich, *et al., Phys. Rev. B* **43,** 7852 (1991).
12. K. K. Singh, P. Ganguly, and J. B. Goodenough, *J. Solid State Chem.* **52,** 254 (1984).
13. M. Sayer, R. Chen, R. Fletcher, and A. Mansingh, *J. Phys. C.* **8,** 2059 (1975); M. Sayer and P. Odier, *J. Solid State Chem.* **67,** 26 (1987).
14. J. Gopalakrishnan, G. Colsmann, and B. Reuter, *J. Solid State Chem.* **22,** 145 (1977).
15. B. W. Arbuckle, K. V. Ramanujachary, Z. Zhang, and M. Greenblatt, *J. Solid State Chem.* **88,** 278 (1990).
16. See, for example, M. Tallan (Ed.), "Electrical Conductivity in Ceramics and Glass," Part B, Dekker, New York (1974).
17. J. B. Webb and M. Sayer, *J. Phys. C* **9,** 4151 (1976).
18. N. F. Mott and E. A. Davis, "Electronic Processes in Non-crystalline Materials," The International Series of Monographs on Physics, Oxford Univ. Press, Oxford (1971).
19. J. M. Bassat, F. Gervais, P. Odier, and J. P. Loup, *Mater. Sci. Eng. B* **3,** 507 (1989).
20. A. C. Smith, J. F. Janak, and R. D. Adler, *in* "Electronic Conduction in Solids," McGraw–Hill, New York (1967).
21. T. H. Geballe and G. W. Hull, *Phys. Rev.* **94,** 1134 (1954) and **98,** 940 (1955).
22. M. Schluter and M. S. Hybersten, *Physica C* **162–164,** 583 (1989); M. Schluter, M. S. Hybersten, and N. E. Christensen, *Physica C* **153,** 1217 (1989) and *Phys. Rev. B* **39,** 9028 (1989); A. K. McMahan, R. M. Martin and S. Satpathy, *Phys. Rev. B* **38,** 6650 (1988).
23. P. Kuiper, G. Kriuzinga, J. Ghijsen, G. A. Sawatzky, and H. Verweij, *Phys. Rev. Lett.* **62,** 221 (1989).
24. M. Medarde, X. Batlle, X. Granados, X. Obradors, J. Rodríguez-Carvajal, J. Fontcuberta, M. Vallet, J. González-Calvet, J. Alonso, M. J. Sayagués, J. L. Martínez, and A. Fontaine, *in* "Electronic Properties of High Temperature Superconductors and Related Compounds" (H. Kuzmany *et al.*, Eds.), Springer Series in Solid-State Sciences, Vol. 99, Springer-Verlag, Berlin (1990).
25. P. Lacorre, J. B. Torrance, J. Pannetier, A. T. Nazzal, P. W. Wang, and T. C. Huang, *J. Solid State Chem.* **91,** 225 (1991); J. B. Torrance, P. Lacorre, A. T. Nazzal, E. J. Ansaldo, and Ch. Niedermayer, *Phys. Rev. B* **45,** 8209 (1992).
26. J. L. García-Muñoz, J. Rodríguez-Carvajal and P. Lacorre, *Phys. Rev.*, in press.
27. Th. Strangfeld, K. Westerholt, and H. Bach, *Physica C* **183,** 1 (1991).